FULL PAPER DOI: 10.1002/adsc.201901252

Advanced Synthesis & Catalysis

Check for updates

Very Important Publication

Engineering the Active Site of an (*S*)-Selective Amine Transaminase for Acceptance of Doubly Bulky Primary Amines

Henrik Land,[a, b] Federica Ruggieri,[a] Anna Szekrenyi,[c] Wolf-Dieter Fessner,[c] and Per Berglund[a,*]

[a] KTH Royal Institute of Technology, School of Engineering Sciences in Chemistry, Biotechnology and Health (CBH), Department of Industrial Biotechnology, AlbaNova University Center, SE-106 91, Stockholm, Sweden
Tel: +46 8 790 7037
E-mail: perbe@kth.se

[b] Uppsala University, Department of Chemistry-Ångström Laboratory, Molecular Biomimetics, Box 523, SE-751 20, Uppsala, Sweden

[c] Technische Universität Darmstadt, Institut für Organische Chemie und Biochemie, Alarich-Weiss-Str. 4, 64287 Darmstadt, Germany

Manuscript received: September 27, 2019; Revised manuscript received: November 20, 2019;
Version of record online: December 11, 2019

This work was dedicated to Marko Mihovilovic on the occasion of his 50th anniversary

Supporting information for this article is available on the WWW under https://doi.org/10.1002/adsc.201901252

Abstract: A protein engineering approach for expanding the substrate scope of the (*S*)-selective *Chromobacterium violaceum* amine transaminase is presented. Amino acid residues in the small binding pocket of the active site were targeted in order to increase the pocket size for acceptance of primary amines bearing two bulky groups. A highly sensitive fluorescence assay was then used to evaluate the generated enzyme variants for their activity towards propyl- and benzyl-substituted screening substrates. The best variant, L59A/F88A, was successfully applied in the kinetic resolution of 1,2-diphenylethylamine using different conditions and substrate loadings. The variant L59A/F88A generated enantiomerically pure (*R*)-1,2-diphenylethylamine with *ee* > 99% under all tested conditions. The variant also holds great promise for synthesis of hydrophobic compounds as it shows optimum activity when 20-30% (v/v) DMSO is applied as cosolvent. The variant L59A/F88A provides a great addition to the available catalyst toolbox for synthesis of chiral amines, as it is the first published (*S*)-selective amine transaminase showing activity towards benzyl-substituted primary amines.

Keywords: Biocatalysis; Aminotransferase; Protein engineering; Kinetic resolution; Enzymes

Introduction

Chiral amines represent an important motif in many groups of fine chemicals, including pharmaceuticals[1] and agrochemicals.[2] To ensure high purity of these compounds, synthetic methods need to be very selective towards the desired enantiomer. Many approaches have been developed towards this goal, both chemo- and biocatalytic ones.[3] The field of biocatalytic amine synthesis has been growing rapidly over the last few decades, which has resulted in several viable enzymatic strategies towards enantiomerically pure amines.[4]

One important class of enzymes in the toolbox for chiral amine synthesis are amine transaminases (ATA) which has proven to be useful catalysts both for kinetic resolution of racemic amines and asymmetric synthesis from prochiral ketones. ATAs especially show remark-

able enantioselectivity compared to many chemical catalysts and both (*S*)- as well as (*R*)-selective enzymes are available.[1,5] The ATA active site consists of two binding pockets of different sizes, one large (**L**) and one small (**S**) pocket next to the pyridoxal-5′-phosphate (PLP) cofactor.[6] The **L** pocket accepts larger substrate moieties such as aromatic rings or aliphatic chains. There are even ATAs, both wild-type (WT) and engineered variants, that accept bulky biaryl substituents in the **L** pocket.[7] The S pocket is, however, generally limited to a methyl group or similar small substituents (Figure 1). This considerable spatial difference is the reason for ATA's excellent enantioselectivity, which is a major advantage but it also significantly limits the allowable substrate scope. Since many fine chemicals containing chiral amine motifs present bulky units on both sides of the amine functionality, enzymes that can accept bulkier substrates while maintaining enantioselectivity are of great interest. The possibility to expand the ATA substrate scope by increasing the size of the **S** pocket has previously been explored, but only to some extent. The first example for engineering the size of the **S** pocket was the directed evolution of an (*R*)-selective *Arthrobacter* sp. ATA where the **S** pocket was enlarged to accept a fluorinated benzyl substituent.[8] The **S** pocket of the (*S*)-selective ATA from *Vibrio fluvialis* has been engineered to accept propyl/hydroxymethyl substituents,[9] cyclohexyl/tert-butyl substituents[10] or an isohexyl substituent.[11] Additionally, (*S*)-selective ATAs from *Ruegeria* sp. and *Ochrobactrum anthropi* were recently engineered to accept bulky aromatic substituents and butyl/isopropyl substituents, respectively.[12]

In order to perform catalysis on any particular substrate of choice, a toolbox of different catalysts with individual substrate scope is needed. With this in mind, we envisaged an (*S*)-selective ATA with the ability to accept a benzyl substituent in the **S** pocket, which would yield a catalyst complementary to the previously mentioned (*R*)-selective *Arthrobacter* sp. ATA.[8] When the active site of an enzyme is to be engineered to accept substantially larger substrates, the activity against the target substrate is initially expected to be absent or very low. A highly sensitive assay for detecting activity is therefore required. Previously, we developed a fluorogenic assay for measuring ATA activity based on the transamination of 1-(6-methoxynaphth-2-yl)alkylamines (Scheme 1, **1**). This reaction produces an acetonaphthone product (**2**) that can be measured with high sensitivity due to its strong blue fluorescence.[13] A modular synthetic route towards this group of assay substrates was also developed, allowing the incorporation of structural variations such as the desired benzyl moiety.

Here we present a rational design approach for increasing the size of the **S** pocket of the (*S*)-selective ATA from *Chromobacterium violaceum* (*Cv*-ATA) to accept a bulky benzyl substituent, allowing for the

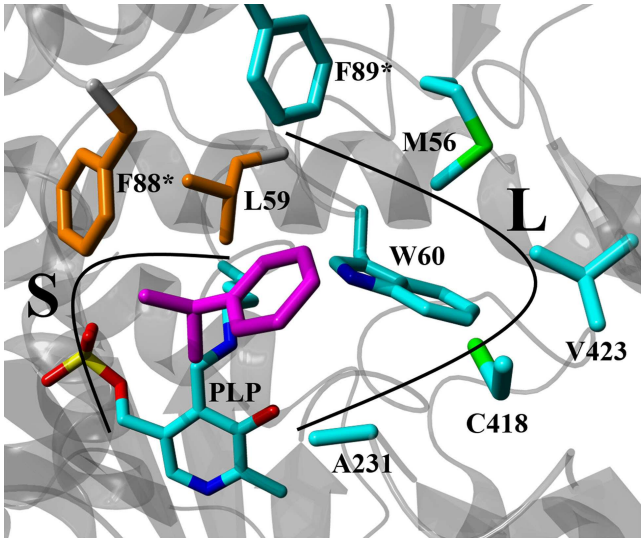

Figure 1. Active site of *Cv*-ATA WT (PDB ID: 4A6T). The active site architecture consisting of a small (**S**) and a large (**L**) binding pocket is illustrated with the binding of (*S*)-1-phenylethylamine (shown in magenta). The two amino acid residues targeted in this study, L59 and F88, are shown in orange. Amino acids from the second subunit are marked with an asterisk (*).

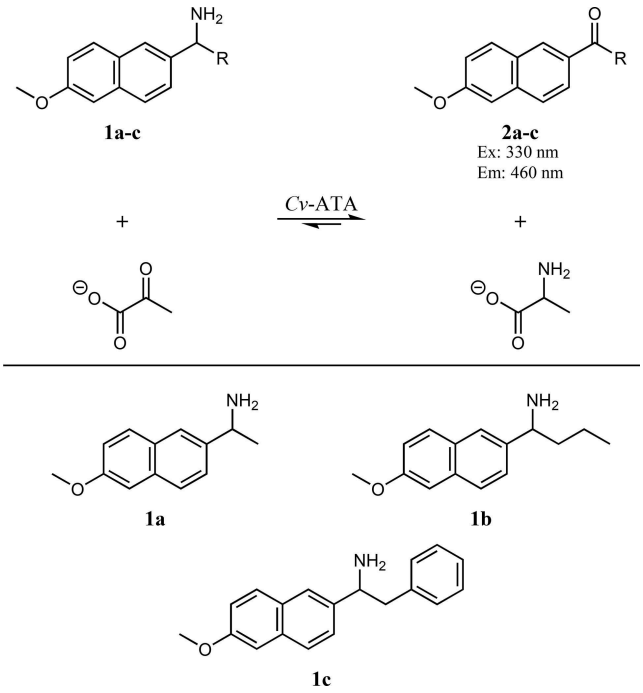

Scheme 1. Screening assay used for evaluation of ATA variants. The ketone product generated upon reaction between the amine substrate and pyruvate can be measured using fluorescence (ex: 330 nm, em: 460 nm).

preparation of enantiomerically pure (*S*)-configured doubly bulky primary amines.

Results and Discussion

Cv-ATA is one of the best known ATAs and characteristics such as substrate scope,[14] reaction kinetics,[13,15] 3D-structure[16] and stability[16a,17] have all been studied in detail. The active site of *Cv*-ATA has also been the subject of several engineering studies.[15b,c,18] With that in mind, *Cv*-ATA was chosen as a starting point for rational design driven expansion of the active site **S** pocket.

Initially, activity of *Cv*-ATA WT against screening substrates **1a–c** was determined using the previously developed fluorescence assay[13] (Scheme 1). Not surprisingly, activity was highest against **1a** that bears the small methyl substituent on the **S** pocket side. Low but detectable activities of 0.33% and 0.084% compared to **1a** were determined for **1b** and **1c**, respectively (Figure 2, Table S1).

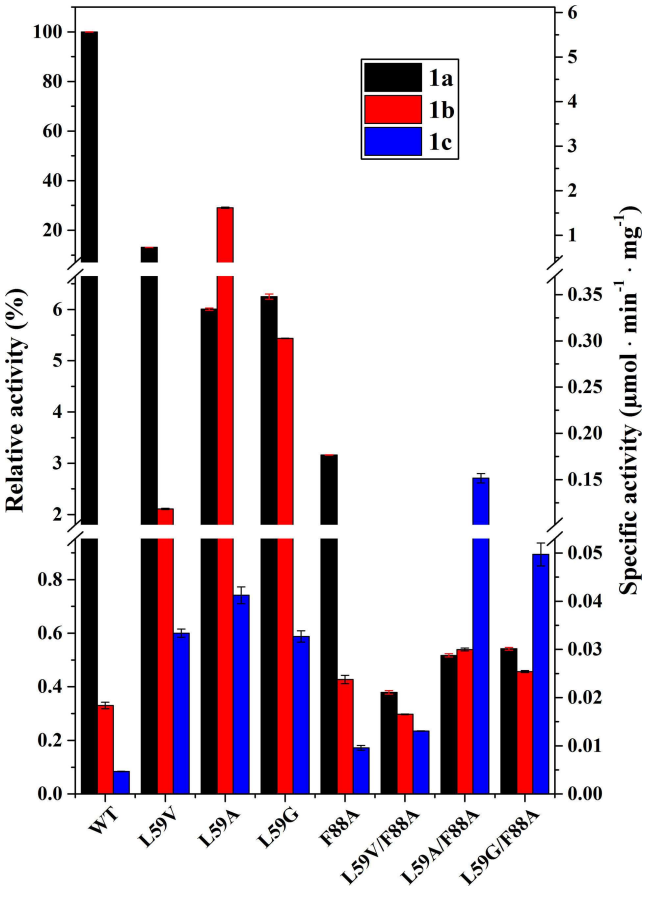

Figure 2. Activities of *Cv*-ATA WT and variants towards screening substrates **1a–c**. Left y-axis: Relative activities where *Cv*-ATA WT activity towards **1a** is set as 100%. Right y-axis: Specific activities expressed as μmol formed **2a–c** min^{-1} mg^{-1} enzyme. For tabulated specific activities, see Table S1.

Next, the active site architecture of *Cv*-ATA WT was investigated in order to identify amino acid residues that could be mutated to increase the size of the **S** pocket without compromising the catalytic machinery. The X-ray crystal structure of *Cv*-ATA WT (PDB ID: 4A6T)[16a] reveals that the **L** pocket in the active site is mainly shaped by residues M56, W60, F89, A231, C418 and V423 (Figure 1). These six residues together form a large cavity where the bulky substituent of the substrate fits nicely. Another critical residue in the **L** pocket is R416, which previously has been shown to flip in and out of the active site in order to make dual substrate recognition between α-carboxylic substrates and bulky uncharged substrates possible.[19] In this crystal structure (4A6T) R416 is adopting a stretched conformation, meaning that it is pointing towards the active site. This residue has therefore been removed from Figure 1 to simulate the corresponding situation when the **L** pocket accepts a bulky uncharged substituent. On the contrary, the **S** pocket is effectively closed off by residues L59 and F88, forming a small cavity opposite to the **L** pocket where only small substituents such as a methyl group fits well.

Amino acid residues L59 and F88 were therefore targeted for site-directed mutagenesis in order to increase the size of the **S** pocket. Position 59 already hosts a medium-sized hydrophobic amino acid (leucine) and was therefore mutated into the only three hydrophobic amino acids that are smaller (valine, alanine and glycine). F88, one of the bulkiest canonical amino acids, was mutated into an alanine. The choice of mutating F88 into alanine instead of glycine (the smallest amino acid) is rationalized by the unpredictable nature of glycine mutations on the secondary structure of the enzyme due to glycine's high rotational freedom.[20] Also, the mutation F88A has previously been successful in enlarging the **S** pocket of *Cv*-ATA.[15b]

The activity of variants L59V, L59A, L59G and F88A against substrates **1a–c** was subsequently determined and all variants showed improved activity against the bulky substrates **1b** and **1c** (Figure 2, Table S1). Especially, variant L59A displayed an impressive 88-fold increased activity against **1b** compared to WT as well as a 8.8-fold improvement against **1c**. All L59 variants were rather similar with regards to **1c** while F88A showed less improvement. In an effort to further increase the size of the **S** pocket, all three L59 variants were subsequently combined with the F88A mutation. All three double-mutants showed decreased activity against **1b** and L59V/F88A had reduced activity against **1c**. However, L59G/F88A caused 11-fold increased activity against **1c** compared to WT and L59A/F88A even displayed a 32-fold improvement (Figure 2, Table S1). This shows that the double-mutant L59A/F88A is the best variant for

accommodation of a benzyl substituent in the **S** pocket. Similar additive effects of mutations have previously been shown when expanding the active site of ATAs.[9,12c] Interestingly, all variants decreased their activity against **1 a**. This can be explained by a decrease in direct interactions between the methyl group and the **S** pocket residues as the pocket enlarges. A similar pattern can be seen with **1 b** where activity first increases with an increasing pocket size but then decreases as the pocket is further enlarged. (Figure 2).

To further examine the variant L59A/F88A, a biochemical characterization was performed. By measuring relative activities at different pH-values using the acetophenone assay,[21] a pH-optimum of 7.5 for this variant could be determined (Figure 3A). This stands in contrast to the WT that has a pH-optimum of 8.3 (Figure S1).[15a] However, it is not surprising that changes in the active site architecture can affect pH-dependence as it was previously shown that the variant *Cv*-ATA W60C has a significantly altered pH-optimum of 7.0 (Figure S1).[15c]

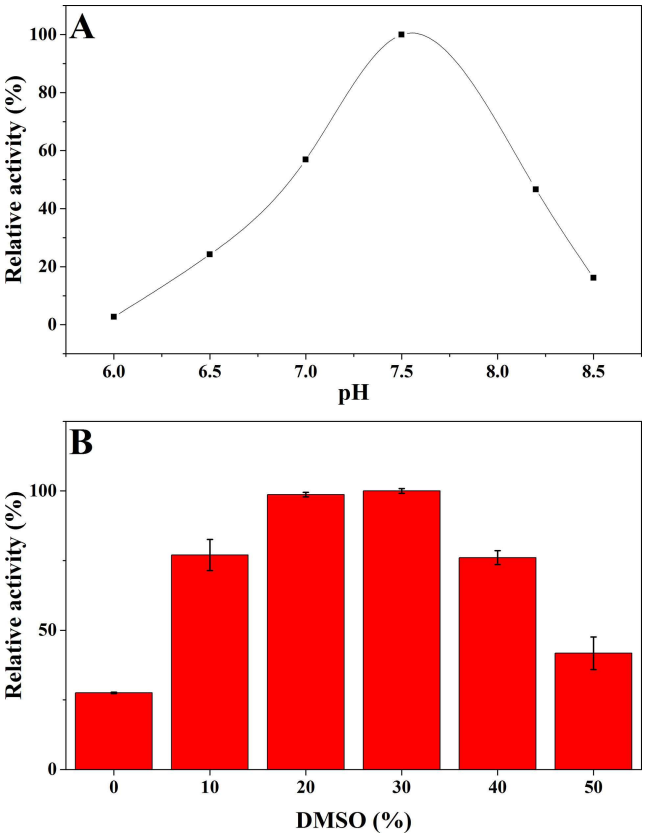

Figure 3. Biochemical characterization of *Cv*-ATA L59A/F88A with regards to (A) pH-optimum and (B) influence of DMSO concentration. The pH-profile was determined with the acetophenone assay at a range of different pH-values. Citrate (pH 6.0 and 6.5) and HEPES (pH 7.0, 7.5 and 8.2) buffers were used at a 50 mM concentration. The DMSO-dependence was determined with the acetophenone assay at a range of different DMSO concentrations (0–50%) in 50 mM HEPES buffer (pH 7.5). Activities are reported as relative to the highest measured activity within each dataset (pH 7.5 and 30% DMSO, respectively).

Due to the hydrophobic nature of the target compounds that variant L59A/F88A was designed to act upon, an investigation on the influence of DMSO on the enzymatic activity was performed. DMSO is a commonly applied co-solvent in biocatalysis when the solubility of hydrophobic substrates needs to be increased and it is one of the best tolerated co-solvents for various enzyme types, as recently demonstrated in a systematic stability study involving eight common water-miscible organic solvents.[22] Other examples of co-solvents applied in ATA-catalyzed reactions include 1,2-dimethoxyethane for solubilization of steroids[23] and deep eutectic solvents for synthesis of biaryl amines.[24] The influence of DMSO on the transamination of (*S*)-1-phenylethylamine and pyruvate was previously reported for *Cv*-ATA WT.[17a] The enzyme displays maximum activity at 0% (v/v) DMSO and a steady activity decrease until it is almost diminished at 50% (v/v) DMSO. Interestingly, the variant L59A/F88A shows a completely different behavior towards DMSO as the activity first increases and reaches a maximum around 20–30% (v/v) DMSO (Figure 3B). Activity then decreases and at 50% (v/v) DMSO, it attains a slightly higher level than for 0% (v/v) DMSO. The reason for this drastic change in DMSO tolerance is yet unknown, but it holds great promise for preparative applications with hydrophobic substrates, both with respect to better substrate solubility but also for increased stability of *Cv*-ATA WT in the presence of elevated concentrations of DMSO.[17a]

The thermostability of variant L59A/F88A was explored by measuring the melting point (T_m, the temperature at which the folded and unfolded enzyme species are at thermodynamic equilibrium) using differential scanning fluorimetry.[25] The results of this analysis show a slight increase in T_m for the L59A/F88A variant (75 °C) as compared to WT (71 °C).

After biochemical characterization, it has been shown that the activity of variant L59A/F88A can be greatly improved by optimizing reaction conditions. As an example, the activity of L59A/F88A towards **1 c** in the fluorescence assay was the highest among all variants, but it was still rather low compared to the activity of *Cv*-ATA WT towards **1 a** (2.7%, Figure 2). However, if the optimized conditions with regards to pH (approximately two times improved activity, Figure 3A) and DMSO concentration (approximately four times improved activity, Figure 3B) were to be applied it can be assumed that the activity of L59A/F88A would be improved approximately eight times, leading to 22% activity towards **1 c** compared to the activity of WT towards **1 a**.

The utility of the engineered L59A/F88A catalyst was evaluated next in the synthesis of 1,2-diphenylethylamine (**3**, Scheme 2). This benzyl-substituted primary amine motif is especially interesting in view of its occurrence in pharmaceutical compounds such as lefetamine,[26] diphenidine[27] and diphenpipenol,[28] which have analgesic and anaesthetic activities. The target compound holds a phenyl-moiety on one side of the amine and a benzyl-moiety on the other side. Even though both substituents are similar in size, they display different conformational rigidity and would point in different directions when bound to the active site of *Cv*-ATA. We hypothesized that the most successful design found for the **S** pocket in the engineered L59A/F88A variant would accommodate the benzyl substituent in preference to the phenyl substituent, thereby resulting in a certain degree of enantioselectivity towards **3**.

An initial exploration of the variant's ability to catalyze the asymmetric synthesis of **3** starting from its prochiral ketone precursor **4** was attempted using the "smart" equilibrium shifting amino donor ortho-xylylenediamine in equimolar (50 mM) amounts.[29] However, it was not successful (Figure S2) and we decided not to pursue this any further. The reason for the low reactivity of **4** might be due to its low water solubility or due to thermodynamic stabilization by enol formation.

To assess the principal activity and enantioselectivity of L59A/F88A towards (*R/S*)-**3**, an attempt for kinetic resolution (KR) was pursued instead (Scheme 2) using 1 mM substrate. The results of this exploratory KR (Figure S3) revealed that L59A/F88A completely consumed all (*S*)-**3** while in the WT-catalyzed reaction the remaining amine was still racemic after 1.5 h. This confirms that L59A/F88A is active towards **3** and that it shows high enantioselectivity towards its (*S*)-enantiomer.

In order to explore the performance of the reaction at higher substrate loadings, a KR of **3** catalyzed by the variant L59A/F88A was performed using a slightly

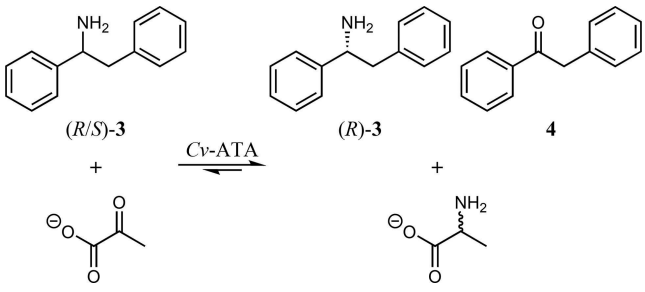

Scheme 2. *Cv*-ATA catalyzed kinetic resolution of 1,2-diphenylethylamine (**3**). Pyruvate is used as amino acceptor, resulting in the generation of alanine, 2-phenylacetophenone (**4**) and enantiomerically pure (*R*)-**3**.

elevated substrate concentration close to the observed solubility limit (5 mM, Figure 4B). Substrate conversion progressed steadily and after 4 h a high enantiomeric excess of the substrate ($ee_S > 99\%$) was accomplished. This stands in contrast to the low activity of *Cv*-ATA WT under the same conditions (Figure 4A).

The addition of 20% (v/v) DMSO as co-solvent was also investigated, thereby exploiting the increased activity of the variant under those conditions (Figure 4C) and also enabling further increase of substrate concentration (20 mM, close to the observed solubility limit in 20% (v/v) DMSO). Again, the reaction proceeded steadily until an $ee_S > 99\%$ was reached already after 2 h.

The applicability of the KR was further explored by adding **3** at concentrations exceeding its solubility limit in aqueous media (100 mM), leading to a non-homogeneous mixture (Figure 4D). However, L59A/F88A tolerated such conditions well and after 4 h, all of (*S*)-**3** was consumed leaving enantiomerically pure (*R*)-**3** ($ee_S > 99\%$).

Conclusion

We have demonstrated a rational design approach towards the successful creation of a *Cv*-ATA variant, L59A/F88A, that is able to kinetically resolve 1,2-diphenylethylamine (**3**) efficiently by accommodating its bulky benzyl substituent in the small **S** pocket of the active site. It is also able to discriminate between a benzyl substituent and a structurally similar phenyl substituent, resulting in high enantioselectivity towards (*S*)-**3**. The use of our previously published, highly sensitive fluorescent screening method[13] with specifically designed substrates (Scheme 1) enabled a substrate walking approach where very low starting activities could be detected and subsequently improved by rational protein engineering. The variant L59A/F88A also displayed interesting biochemical properties as its alkaline pH optimum was displaced by almost one unit towards an almost neutral pH. Its behaviour towards the water-miscible co-solvent DMSO also showed a drastic change. While the WT enzyme has its maximum activity at 0% (v/v) DMSO with a steady decrease in activity as the concentration increases, the variant shows an activity optimum at 20% (v/v) DMSO. This shows great promise for future application as DMSO is commonly used to increase solubility of hydrophobic substrates. Finally, the generated variant L59A/F88A shows great promise in the resolution of racemic **3** for generation of enantiomerically pure (*R*)-**3** with a highest tested substrate loading of 100 mM (20 g/L).

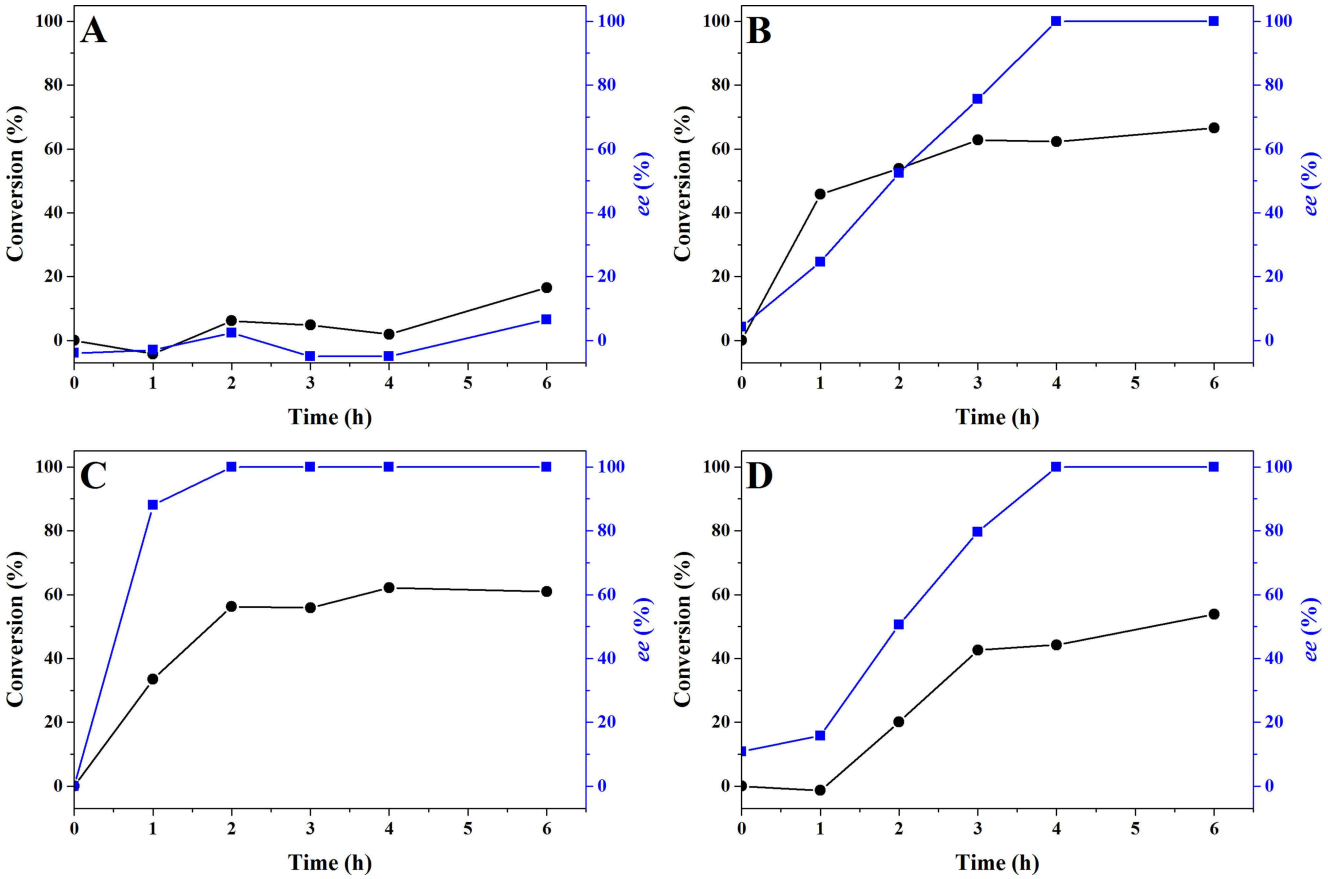

Figure 4. *Cv*-ATA catalyzed kinetic resolution of 1,2-diphenylethylamine (**3**). (A) 5 mM **3**, 7.5 mM pyruvate, 0% (v/v) DMSO, 0.5 mg *Cv*-ATA WT. (B) 5 mM **3**, 7.5 mM pyruvate, 0% (v/v) DMSO, 0.5 mg *Cv*-ATA L59A/F88A. (C) 20 mM **3**, 30 mM pyruvate, 20% (v/v) DMSO, 2 mg *Cv*-ATA L59A/F88A. (D) 100 mM **3**, 200 mM pyruvate, 0% (v/v) DMSO, 5.4 mg *Cv*-ATA L59A/F88A, magnetic stirring. All reactions were performed at room temperature in 3 ml reaction volumes and under shaking unless otherwise specified. Conversion (●) and *ee* (■).

Experimental Section

Materials

All chemicals were purchased from Sigma-Aldrich and used without further purification, unless otherwise stated. The HisPrep column used for enzyme purification and the PD10 desalting columns were purchased from GE Healthcare Life Science (Sweden).

Site-Directed Mutagenesis

The *Cv*-ATA gene was previously inserted into pET-28a(+) with a N-terminal His_6-tag.[15a] Site-directed mutagenesis was performed by the Quick Change method with modifications according to Zheng *et. al.*, using Phusion High-Fidelity DNA Polymerase from Thermo Fisher. The primers used are listed below, with the mutations indicated in lower case:

Cv-ATA_L59G_f:

5′-GCAGGTggtTGGTGTGTTAATGTTG-3′

Cv-ATA_L59G_r:

5′-CACCAaccACCTGCCATACCATC-3′

Cv-ATA_L59 A_f:

5′-CAGGTgcaTGGTGTGTTAATGTTG-3′

Cv-ATA_L59 A_r:

5′-CACCAtgcACCTGCCATACC-3′

Cv-ATA_L59 V_f:

5′-CAGGTgttTGGTGTGTTAATGTTG-3′

Cv-ATA_L59 V_r:

5′-CACCAaacACCTGCCATACC-3′

Cv-ATA_F88 A_f:

5′-GTTTTATAATACCgccTTTAAAACCACCC-3′

Cv-ATA_F88 A_r:

5′-GGTTTTAAAggcGGTATTATAAAACGGC-3′

Enzyme Expression and Purification

Expression of *Cv*-ATA WT and variants was performed by inoculating 20 mL LB-medium (50 µg/mL kanamycin) with *Escherichia coli* (*E. coli*) BL21 (DE3) cells containing the *Cv*-ATA encoding plasmid. The culture was incubated at 37 °C and 210 rpm overnight. 180 mL LB-medium (50 µg/mL kanamycin and 0.4 mM isopropyl β-D-1-thiogalactopyranoside (IPTG)) was then inoculated with the overnight culture and incubated at 25 °C and 140 rpm for 24 h. After expression, the cells were harvested by centrifugation (8000 rpm for 15 min). The cell pellet was dissolved in Immobilized Metal ion Affinity Chromatography (IMAC) binding buffer (sodium phosphate buffer (20 mM, pH 7.4) and NaCl (0.5 M)) and cells were disrupted by sonication. Cell debris was removed by centrifugation (20000 rpm for 15 min) and the supernatant was collected and filtered (0.45 µm). The enzyme was then purified by IMAC using a 5 mL HisPrep column according to the manufacturers' protocol. Pyridoxal-5′-phosphate (PLP) was added in an excess (1 mM) and the solution was incubated in room temperature for 30 minutes. Finally, a buffer exchange to HEPES buffer (50 mM, pH 7.5 or 8.2) was performed by running the solution through a PD-10 column according to the manufacturers' protocol. The enzyme solution was stored at 4 °C. Enzyme concentrations were determined according to Pace *et al.*[30]

Larger scale *Cv*-ATA L59 A/F88 A expression and purification was performed in 1 L TB medium supplemented with antibiotic (50 µg/mL kanamycin) starting from 10 ml of overnight preculture. Expression was induced at OD_{600} = 0.8 with 0.3 mM IPTG and carried out at 15 °C in the dark over 24 h and 150 rpm agitation. Cells were harvested by centrifugation (4 °C, 4000 xg, 30 min), resuspended in 50 mM HEPES pH 7.5, 10 mM imidazole and sonicated on ice at medium intensity with 50% pulses. The lysate was clarified by centrifugation (4 °C, 30000 xg, 40 min) and filtration (0.45 µm) prior to loading on pre-equilibrated 5 ml Ni-NTA cartridges (GE Healthcare). The target protein was eluted in a linear gradient to 0.5 M imidazole in 40 min at a flow rate of 2.5 ml/min. The fractions containing the target were pooled together, supplemented with PLP (1.2 mg) and stored overnight at 4 °C in the dark. The protein was then buffer-exchanged in 50 mM HEPES pH 7.5 using an Amicon Ultra Centrifugal Filter (cut-off 30 kDa, Merck Millipore Ltd.). Protein aliquots were flash frozen in liquid nitrogen and stored at −80 °C until use.

Screening Substrate 1 a–c Synthesis

Screening substrates **1 a–b** were synthesized according to a previously published protocol.[13] Screening substrate **1 c** was synthesized as follows:

Synthesis of 1-(6-methoxynaphth-2-yl)2-phenylethan-1-ol: In a 100 mL round bottom flask 6-Methoxy-2-naphtaldehyde (2.5 g, 13.5 mmol, 1 eq.) was dissolved in dry tetrahydrofuran (37 mL) under argon atmosphere, and a solution of benzyl magnesium chloride (2.0 M in THF, 7.32 mL, 14,7 mmol, 1.1 eq.) was added slowly at 0 °C. Further benzyl magnesium chloride (1.1 eq.) was added due to incomplete conversion after 2 h, and the mixture was allowed to stir at room temperature for an additional hour. Then the mixture was quenched by the addition of saturated aqueous NH_4Cl (20 mL). After removal of THF under reduced pressure, the aqueous phase was extracted with diethyl ether (3 × 50 mL). The combined organic layers were dried over Na_2SO_4 and the solvent was evaporated. The crude product was recrystallized with n-heptene/toluene to give light yellow crystals (2.07 g, 55%, melting point: 133 °C.

^{1}H NMR (300 MHz, $CDCl_3$): δ = 7.67–7.61 (m, 3H, 8′-, 4′-, 1′-H), 7.38 (dd, *J* = 8.5 Hz, 1.8 Hz, 1H, 3′-H), 7.22–7.12 (m, 5H, Ph), 7.09 (d, *J* = 2.6 Hz, 1H, 7′-H), 7.05 (s, 1H, 5′-H), 4.95 (dd, *J* = 8.1 Hz, 5.1 Hz, 1H, 1-H), 3.84 (s, 3H, OCH_3), 3.07–2.98 (m, 2H, 2-H); ^{13}C NMR ($CDCl_3$, 75 MHz): δ = 157.7 (C-6′), 139.0 (C-1″), 138.1 (C-2′), 134.1 (C-4a′), 129.5 (C-3″ 2×), 129.4 (C-8′), 128.7 (C-3′), 128.5 (C-2″ 2×), 127.0 (C-8a′), 126.6 (C-1′), 124.6 (C-4″), 124.5 (C-4′), 118.9 (C-7′), 105.7 (C-5′), 75.5 (C-1), 55.3 (OCH_3), 46.0 (C-2).

Synthesis of 1-(6-methoxynaphth-2-yl)2-phenylethan-1-one: In a 50 mL round bottom flask the alcohol (2.07 g, 7.33 mmol, 1 eq.) was dissolved in 14 mL acetone and cooled to 0 °C in an ice bath. A solution of CrO_3 (6 mL, 12 mmol, 1.64 eq.) in 30% H_2SO_4 was added to the reaction mixture slowly, so that the temperature remains below 5 °C. When precipitation was observed, more acetone was added. After the mixture was stirred for one hour, it was stopped by quenching the excess oxidant with aqueous $NaHSO_3$. The product was precipitated by addition of water and isolated by filtration, and dissolved in diethyl ether. The solution was washed with 10% Na_2CO_3, water and brine. The organic layer was dried over Na_2SO_4 and the solvent was evaporated under reduced pressure. The crude product was recrystallized from water/ethanol (1:3) to give yellow crystals (1.26 g, 62%), melting point: 115 °C.

^{1}H NMR (300 MHz, $CDCl_3$): δ = 8.41 (s, 1H, 1′-H), 7.98 (dd, *J* = 8.6 Hz, 1.8 Hz, 1H, 4′-H), 7.78 (d, *J* = 9.0 Hz, 1H, 8′-H), 7.69 (d, *J* = 8.7 Hz, 1H, 3′-H), 7.26 (s, 5H, Ph), 7.21–7.08 (m, 2H, 7′-H, 5′-H), 4.32 (s, 2H, 2-H), 3.88 (s, 3H, OCH_3); ^{13}C NMR ($CDCl_3$, 75 MHz): δ = 197.5 (C-1), 160.0 (C-6′), 137.4 (C-1″), 135.0 (C-2′), 132.2 (C-4a′), 131.3 (C-8′), 130.4 (C-8a′), 128.8 (C-3″ 2×), 129.6 (C-3′), 127.9 (C-2″ 2×), 127.3 (C-1′), 127.0 (C-4″), 125.2 (C-4′), 119.8 (C-7′), 105.9 (C-5′), 55.5 (OCH_3), 45.5 (C-2).

Synthesis of 1-(6-methoxynaphthalen-2-yl)-2-phenylethanoneoxime: In a 50 mL round bottom flask the ketone (1.26 g 4.56 mmol, 1 eq.) was dissolved in 33 mL ethanol to this solution a mixture of hydroxylamine hydrochloride (0.48 g, 6.85 mmol, 1.5 eq.) and 0.56 mL pyridine (6.85 mmol, 1.5 eq.) was added. The reaction mixture was stirred at 60 °C for 16 h. A change in colour, yellow to orange was observed. The solvent was evaporated under reduced pressure, and the residue dissolved in 10 mL dichloromethane. The dissolved product was washed with water (2 × 10 mL) and brine (1 × 10 mL). The organic phase was dried with Na_2SO_4 and the solvent removed under reduced pressure. The obtained product was purified by flash column chromatography on silica gel (cyclohexane/ethyl acetate 10–20%) to give orange crystals (1.09 g, 82%).

^{1}H NMR (300 MHz, $CDCl_3$): δ = 8.50 (s, 1H, 1′-H), 8.07 (dd, *J* = 8.7 Hz, 1.8 Hz,1H, 4′-H), 7.90 (d, *J* = 8.9 Hz, 1H, 8′-H), 7.78 (d, *J* = 8.6 Hz, 1H, 3′-H), 7.39–7.31 (m, 5H, Ph), 7.29–7.16 (m, 2H, 7′-H, 5′-H), 4.41 (s, 2H, 2-H), 3.96 (s, 3H, OCH_3); ^{13}C NMR ($CDCl_3$, 75 MHz): δ = 197.3 (C-1), 159.9 (C-6′), 137.3 (C-2′), 134.9 (C-4a′), 132.1 (C-8′), 131.2 (C-8a′), 130.3

(C-3′), 129.5 (C-3″ 2×), 128.7 (C-2″ 2×), 127.8 (C-1′), 127.2 (C-1″), 126.8 (C-4″), 125.0 (C-4′), 119.7 (C-7′), 105.8 (C-5′), 55.4 (OCH_3), 45.4 (C-2).

Synthesis of 1-(6-methoxynaphthalen-2-yl)-2-phenylethanamine: The oxime (1.09 g, 3.74 mmol, 1 eq.) was dissolved in 50 mL acetic acid and 3 mL water. The mixture was heated to 110 °C and activated Zn (3.4 g, 52 mmol, 13.9 eq.) was added portion wise to the reaction over the course of 25 minutes. After a total of 2 h reaction time the mixture was cooled down and neutralized with a saturated solution of $NaHCO_3$. The product was extracted with dichloromethane (3×50 mL) and the combined organic layers were dried over Na_2SO_4. The solvent was removed under reduced pressure to give pale yellow crystals (892 mg, 86%).

^{1}H NMR (300 MHz, $CDCl_3$): δ = 7.77–7.72 (m, 3H, 1′-, 3′-, 4′-H), 7.51 (dd, *J* = 8.4 Hz, 1.8 Hz, 1H, 7′-H), 7.38–7.17 (m, 7H, Ph, 8′-H, 5′-H), 4.36 (dd, *J* = 8.8 Hz, 5.0 Hz, 1H, 1-H), 3.94 (s, 3H, OCH_3), 3.16–2.90 (m, 2H, 2-H); ^{13}C NMR ($CDCl_3$, 75 MHz): δ = 157.5 (C-6′), 140.8 (C-1″), 139.1 (C-2′), 133.9 (C-4a′), 129.4 (C-3″ 2×), 129.3 (C-8′), 128.9 (C-8a′), 128.5 (C-2″ 2×), 127.0 (C-3′), 126.4 (C-1′),125.6 (C-4″), 124.7 (C-4′), 118.8 (C-7′), 105.7 (C-5′), 57.6 (C-1), 55.3 (OCH_3), 46.4 (C-2).

Synthesis of 1-(6-methoxynaphthalen-2-yl)-2-phenylethanammonium chloride: In a 250 mL round bottom flask the amine (892 mg, 3.2 mmol, 1 eq.) was dissolved in 125 mL dry diethyl ether under argon atmosphere. HCl gas was bubbled through the solution until salt precipitation could be observed. The product was filtered and washed with ether, and the residual solvent was removed under reduced pressure to give white crystals (640 mg, 64%), melting point: 275 °C (decomposition).

^{1}H NMR (300 MHz, $CDCl_3$): δ = 7.85–7.73 (m, 3H, 1′-, 3′-, 4′-H), 7.51 (d, *J* = 8.6 Hz, 1H, 7′-H), 7.28–7.14 (m, 7H, Ph, 5′-, 8′-H,), 4.67 (dd, *J* = 9.1 Hz, 6.1 Hz, 1H, 1-H), 3.89 (s, 3H, OCH_3), 3.49–3.30 (m, 2H, 2-H); ^{13}C NMR ($CDCl_3$, 75 MHz): δ = 159.9 (C-6′), 137.0 (C-1″), 136.3 (C-2′), 132.6 (C-4a′), 130.6 (C-8′), 130.5 (C-3″ 2×), 130.0 (C-8a′), 129.7 (C-2″ 2×), 129.0 (C-4″), 128.2 (C-3′), 128.2 (C-1′), 125.9 (C-4′), 120.6 (C-7′), 106.7 (C-5′), 58.6 (C-1), 55.9 (OCH_3), 41.9 (C-2).

All NMR spectra were recorded on a Bruker AX300 spectrometer

Enzyme Activity Assays

Fluorescence assay: The fluorescence assay was performed as previously described. Substrate concentrations were set to 1 mM **1 a–c** and 4.5 mM sodium pyruvate. Data was fitted using the BMG CLARIOstar software. Every measurement was performed in duplicate.

Acetophenone assay: The acetophenone assay[21] was performed using 5 mM (*S*)-1-phenylethylamine and 5 mM sodium pyruvate in different buffers at room temperature. Acetophenone formation was monitored at 245 nm using a Cary50 UV/Vis spectrophotometer.

Biochemical Characterization

pH-dependence: The pH-profile of *Cv*-ATA L59A/F88A was determined with the acetophenone assay at a range of different pH-values. Citrate (pH 6.0 and 6.5) and HEPES (pH 7.0, 7.5 and 8.2) buffers were used at a 50 mM concentration.

DMSO-dependence: The DMSO-dependence of *Cv*-ATA L59A/F88A was determined with the acetophenone assay at a range of different DMSO concentrations (0–50%) in 50 mM HEPES buffer (pH 7.5). Every measurement was performed in duplicate.

Differential scanning fluorimetry: Melting temperature (T_m) values were measured using differential scanning fluorimetry (DSF).[25] The measurement was performed on a CFX96 real-time PCR detection system and C1000 thermal cycler at 569 nm. The reaction sample (20 µL) consisted of 1 mg/mL enzyme and 5× SYPRO Orange protein gel stain (Sigma Aldrich, S5692) in HEPES buffer (50 mM, pH 7.5). The temperature range was set to 25–95 °C, with an increase of 1 °C/min. Every measurement was performed in duplicate.

Kinetic Resolutions

Kinetic resolutions were performed in a 3 mL reaction volume in 500 mM HEPES buffer (pH 7.5, 0 or 20% (v/v) DMSO). Substrate concentrations were 5–100 mM **3** and 7.5–200 mM sodium puruvate. 0.5, 2.0 or 5.4 mg enzyme was used. See Figure 4 for specific conditions regarding each reaction. Reactions were run for 6 h and samples were collected regularly for analysis.

Conversion was analyzed using a Hewlett Packard 5890 gas chromatograph (GC) equipped with an Agilent CP-Sil 5 CB column (30 m×0.25 mm×0.25 µm) and a flame ionization detector (FID). Consumption of amine substrate was determined with the following temperature gradient: starting temperature 120 °C, 10 °C/min to 130 °C (hold 2 min), 5 °C/min to 180 °C, 25 °C/min to 300 °C (hold 2 min). Retention times: **3** (12.1 min), **4** (12.7 min). Injector temperature was 275 °C and detector temperature was 300 °C. Sample preparation for GC analysis was performed by collecting 100 µL reaction sample. 10 µL NaOH (1 M) was added and the amine was extracted into 200 µL hexane. The organic phase was dried over anhydrous Na_2SO_4 and the sample was then centrifuged and analyzed on GC.

Enantiomeric excess was analyzed with normal phase HPLC on a Hewlett Packard 1100 liquid chromatography system using a Chiralcel OD–H column. As mobile phase, hexane:2-propanol:DEA (90:10:0.1) was used at a flow of 1 mL/min. Amine absorbance was detected at 215 nm. Retention times: (*R*)-**3** (8 min), (*S*)-**3** (11 min). Sample preparation for HPLC was performed by collecting 100 µL reaction sample. 10 µL HCl (1 M) was added and the ketone was removed by extraction to hexane. 20 µL NaOH (1 M) was added to the aqueous phase and the amine was extracted into 200 µL hexane. The organic phase was dried over anhydrous Na_2SO_4 and the sample was then centrifuged and evaporated. Amine was redissolved in 100 µL hexane:2-propanol (90:10). 10 µL was then injected.

Acknowledgements

Dr Luuk van Langen, Viazym, Delft, NL, is gratefully acknowledged for scientific advice. This project has received funding through the German Federal Ministry of Education and Research (BMBF) under Grant Agreement No 031B0595 (Tralaminol; to WDF) and the initiative ERA CoBioTech, which has received funding from the European Union's Horizon 2020 Research and Innovation Programme under grant agreement No 722361.

References

[1] S. A. Kelly, S. Pohle, S. Wharry, S. Mix, C. C. R. Allen, T. S. Moody, B. F. Gilmore, *Chem. Rev.* **2018**, *118*, 349–367.

[2] P. Jeschke, *Pest Manage. Sci.* **2018**, *74*, 2389–2404.

[3] T. C. Nugent, *Chiral Amine Synthesis: Methods, Developments and Applications*, John Wiley & Sons, Inc., **2010**.

[4] a) D. Ghislieri, N. J. Turner, *Top. Catal.* **2014**, *57*, 284–300; b) H. Kohls, F. Steffen-Munsberg, M. Höhne, *Curr. Opin. Chem. Biol.* **2014**, *19*, 180–192; c) G. Grogan, *Curr. Opin. Chem. Biol.* **2018**, *43*, 15–22.

[5] a) F. Guo, P. Berglund, *Green Chem.* **2017**, *19*, 333–360; b) A. Gomm, E. O'Reilly, *Curr. Opin. Chem. Biol.* **2018**, *43*, 106–112.

[6] a) J.-S. Shin, B.-G. Kim, *J. Org. Chem.* **2002**, *67*, 2848–2853; b) B.-K. Cho, H.-Y. Park, J.-H. Seo, J. Kim, T.-J. Kang, B.-S. Lee, B.-G. Kim, *Biotechnol. Bioeng.* **2008**, *99*, 275–284; c) M. Höhne, S. Schätzle, H. Jochens, K. Robins, U. T. Bornscheuer, *Nat. Chem. Biol.* **2010**, *6*, 807–813.

[7] a) D. F. A. R. Dourado, S. Pohle, A. T. P. Carvalho, D. S. Dheeman, J. M. Caswell, T. Skvortsov, I. Miskelly, R. T. Brown, D. J. Quinn, C. C. R. Allen, L. Kulakov, M. Huang, T. S. Moody, *ACS Catal.* **2016**, *6*, 7749–7759; b) A. W. H. Dawood, J. Bassut, R. O. M. A. de Souza, U. T. Bornscheuer, *Chem. Eur. J.* **2018**, *24*, 16009–16013; c) A. Telzerow, J. Paris, M. Håkansson, J. González-Sabín, N. Ríos-Lombardía, M. Schürmann, H. Gröger, F. Morís, R. Kourist, H. Schwab, K. Steiner, *ACS Catal.* **2019**, *9*, 1140–1148.

[8] C. K. Savile, J. M. Janey, E. C. Mundorff, J. C. Moore, S. Tam, W. R. Jarvis, J. C. Colbeck, A. Krebber, F. J. Fleitz, J. Brands, P. N. Devine, G. W. Huisman, G. J. Hughes, *Science* **2010**, *329*, 305–309.

[9] A. Nobili, F. Steffen-Munsberg, H. Kohls, I. Trentin, C. Schulzke, M. Höhne, U. T. Bornscheuer, *ChemCatChem* **2015**, *7*, 757–760.

[10] M. Genz, O. Melse, S. Schmidt, C. Vickers, M. Dörr, T. van den Bergh, H.-J. Joosten, U. T. Bornscheuer, *ChemCatChem* **2016**, *8*, 3199–3202.

[11] K. S. Midelfort, R. Kumar, S. Han, M. J. Karmilowicz, K. McConnell, D. K. Gehlhaar, A. Mistry, J. S. Chang, M. Anderson, A. Villalobos, J. Minshull, S. Govindarajan, J. W. Wong, *Protein Eng. Des. Sel.* **2013**, *26*, 25–33.

[12] a) I. V. Pavlidis, M. S. Weiss, M. Genz, P. Spurr, S. P. Hanlon, B. Wirz, H. Iding, U. T. Bornscheuer, *Nat. Chem.* **2016**, *8*, 1076–1082; b) S.-W. Han, E.-S. Park, J.-Y. Dong, J.-S. Shin, *Appl. Environ. Microbiol.* **2015**, *81*, 6994–7002; c) H.-G. Kim, S.-W. Han, J.-S. Shin, *Adv. Synth. Catal.* **2019**, *361*, 2594–2606.

[13] T. Scheidt, H. Land, M. Anderson, Y. Chen, P. Berglund, D. Yi, W.-D. Fessner, *Adv. Synth. Catal.* **2015**, *357*, 1721–1731.

[14] a) U. Kaulmann, K. Smithies, M. E. B. Smith, H. C. Hailes, J. M. Ward, *Enzyme Microb. Technol.* **2007**, *41*, 628–637; b) D. Pressnitz, C. S. Fuchs, J. H. Sattler, T. Knaus, P. Macheroux, F. G. Mutti, W. Kroutil, *ACS Catal.* **2013**, *3*, 555–559; c) N. G. Schmidt, R. C. Simon, W. Kroutil, *Adv. Synth. Catal.* **2015**, *357*, 1815–1821; d) N. Richter, R. C. Simon, H. Lechner, W. Kroutil, J. M. Ward, H. C. Hailes, *Org. Biomol. Chem.* **2015**, *13*, 8843–8851.

[15] a) K. E. Cassimjee, M. S. Humble, V. Miceli, C. G. Colomina, P. Berglund, *ACS Catal.* **2011**, *1*, 1051–1055; b) M. S. Humble, K. E. Cassimjee, V. Abedi, H.-J. Federsel, P. Berglund, *ChemCatChem* **2012**, *4*, 1167–1172; c) K. E. Cassimjee, M. S. Humble, H. Land, V. Abedi, P. Berglund, *Org. Biomol. Chem.* **2012**, *10*, 5466–5470.

[16] a) M. S. Humble, K. E. Cassimjee, M. Håkansson, Y. R. Kimbung, B. Walse, V. Abedi, H.-J. Federsel, P. Berglund, D. T. Logan, *FEBS J.* **2012**, *279*, 779–792; b) C. Sayer, M. N. Isupov, A. Westlake, J. A. Littlechild, *Acta Crystallogr. Sect. D* **2013**, *69*, 564–576.

[17] a) S. Chen, H. Land, P. Berglund, M. S. Humble, *J. Mol. Catal. B* **2016**, *124*, 20–28; b) S. Chen, P. Berglund, M. S. Humble, *Mol. Cancer* **2018**, *446*, 115–123; c) H. Land, J. C. Campillo-Brocal, M. S. Humble, P. Berglund, *ChemBioChem* **2019**, *20*, 1297–1304.

[18] D. Deszcz, P. Affaticati, N. Ladkau, A. Gegel, J. M. Ward, H. C. Hailes, P. A. Dalby, *FEBS J.* **2015**, *282*, 2512–2526.

[19] F. Steffen-Munsberg, C. Vickers, A. Thontowi, S. Schätzle, T. Meinhardt, M. S. Humble, H. Land, P. Berglund, U. T. Bornscheuer, M. Höhne, *ChemCatChem* **2013**, *5*, 154–157.

[20] a) B. X. Yan, Y. Q. Sun, *J. Biol. Chem.* **1997**, *272*, 3190–3194; b) B. L. de Groot, D. M. van Aalten, R. M. Scheek, A. Amadei, G. Vriend, H. J. Berendsen, *Protein J.* **1997**, *29*, 240–251.

[21] S. Schätzle, M. Höhne, E. Redestad, K. Robins, U. T. Bornscheuer, *Anal. Chem.* **2009**, *81*, 8244–8248.

[22] A. O. Magnusson, A. Szekrenyi, H. J. Joosten, J. Finnigan, S. Charnock, W. D. Fessner, *FEBS J.* **2019**, *286*, 184–204.

[23] N. Richter, R. C. Simon, W. Kroutil, J. M. Ward, H. C. Hailes, *Chem. Commun.* **2014**, *50*, 6098–6100.

[24] J. Paris, A. Telzerow, N. Ríos-Lombardía, K. Steiner, H. Schwab, F. Morís, H. Gröger, J. González-Sabín, *ACS Sustainable Chem. Eng.* **2019**, *7*, 5486–5493.

[25] F. H. Niesen, H. Berglund, M. Vedadi, *Nat. Protoc.* **2007**, *2*, 2212–2221.

[26] C. S. D. Wink, G. M. J. Meyer, J. Zapp, H. H. Maurer, *Anal. Bioanal. Chem.* **2015**, *407*, 1545–1557.
[27] C. S. D. Wink, J. A. Michely, A. Jacobsen-Bauer, J. Zapp, H. H. Maurer, *Drug Test. Anal.* **2016**, *8*, 1005–1014.
[28] K. Natsuka, H. Nakamura, Y. Nishikawa, T. Negoro, H. Uno, H. Nishimura, *J. Med. Chem.* **1987**, *30*, 1779–1787.
[29] A. P. Green, N. J. Turner, E. O'Reilly, *Angew. Chem. Int. Ed.* **2014**, *53*, 10714–10717.
[30] C. N. Pace, F. Vajdos, L. Fee, G. Grimsley, T. Gray, *Protein Sci.* **1995**, *4*, 2411–2423.

